

Helimagnetism in a disordered and geometrically frustrated quantum spin chain.

T. Masuda,¹ A. Zheludev,¹ A. Bush,² M. Markina,³ and A. Vasiliev³

¹Condensed Matter Sciences Division, Oak Ridge National Laboratory, Oak Ridge, TN 37831-6393, USA.

²Moscow Institute of Radiotechnics, Electronics and Automation, Moscow 117464, Russia.

³Low Temperature Physics Department, Moscow State University, Moscow 119992, Russia.

(Dated: November 19, 2018)

Neutron diffraction and bulk measurements are used to determine the nature of the low-temperature ordered state in a $S = 1/2$ spin-chain compound with competing interactions. The magnetic structure is found to be helimagnetic, with a propagation vector $(0.5, \zeta, 0)$, $\zeta = 0.174$. The nearest-neighbor exchange constant and frustration ratio are estimated to be $J = 5.8$ meV and $J_2/J_1 = 0.29$, respectively. For idealized spin chains these parameter values would signify a gapped spin-liquid ground state. Long-range ordering is attributed to intrinsic non-stoichiometry.

In recent years the focus in quantum and low-dimensional magnetism has shifted from the simplest nearest-neighbor chain models to more complex spin networks, effects of impurities, disorder, and inter-chain coupling. Of particular interest are cases that involve strong geometric frustration of interactions. Any of these effects may either enhance or suppress quantum fluctuations, and thus play a crucial role in determining the ground state and magnetic properties. Even the simplest frustrated models, such as the $S = 1/2$ spin chain with competing nearest-neighbor (nn) next-nearest-neighbor (nnn) antiferromagnetic (AF) interactions, have a rich phase diagram that includes both gapped and quantum-critical gapless phases [1]. Among the latter is, for example, a unique disordered chiral state [2], which is all that quantum fluctuations preserve of helimagnetism, realized in the classical version of the model. The challenge is to find experimental realizations of frustrated-chain constructs, and to understand the effect of disorder, impurities and extended interactions in such materials.

The charge-ordered compound LiCu_2O_2 [3, 4, 5, 6, 7], may, in fact, be just the right model system, featuring $S = 1/2$ chains with strong nnn interactions. Paradoxically, LiCu_2O_2 possesses characteristics of a quantum-disordered “dimer liquid” state, including a gap $\Delta \approx 6$ meV in the magnetic excitation spectrum [6], and yet undergoes at least one magnetic ordering transition, at $T_c \approx 23$ K [3, 6, 7]. The phenomenon is poorly understood, and the key missing pieces of information are the actual structure of the ordered phase and the magnitude of frustration. These issues are topics of an ongoing controversy. μ -SR studies indicate a single complex non-collinear state below $T_c \approx 22.5$ K, with a precursor transition at $T_1 = 24$ K. Some recent bulk measurements [6] point to an *additional* transition at $T^* = 9$ K. None of the published data provide direct information on the frustration ratio of nnn and nn interactions $\alpha = J_2/J_1$. In the present work we show that in samples with thoroughly characterized stoichiometry the transition at T_c results in an *incommensurate* helimagnetic state that persists to low temperatures. We unambiguously determine the frustration ratio, and propose an explanation for the

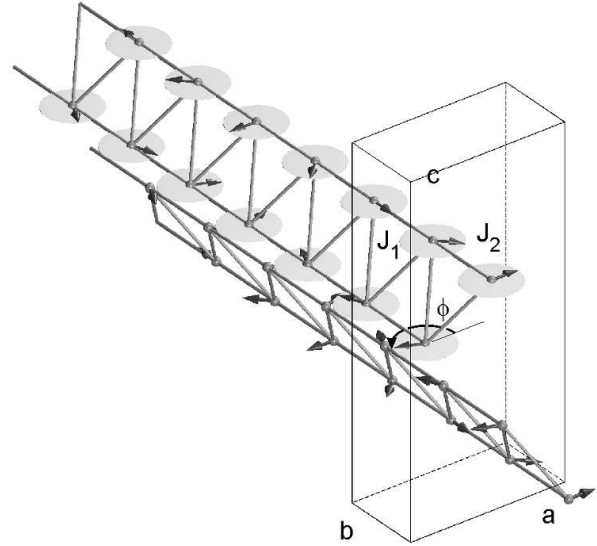


FIG. 1: Crystallographic unit cell of LiCu_2O_2 showing the magnetic Cu^{2+} sites (green balls) and the planar helimagnetic spin structure (arrows) determined in this work.

precursor transition at T_1 . Several alternative mechanisms of magnetic ordering in what “should” have been a quantum-disordered gapped system are proposed.

As discussed in detail in Refs. [6, 7, 8], LiCu_2O_2 contains an equal number of Cu^+ and Cu^{2+} ions in distinct non-equivalent crystallographic positions. The magnetic Cu^{2+} ions carry $S = 1/2$ and form “triangular” two-leg ladders (Fig. 1), which can also be viewed as zig-zag chains with competing nn and nnn interactions, J_{nn} and J_{nnn} , respectively. These chains run along the b axis of the orthorhombic crystal structure, and are well separated from each other by double chains of non-magnetic Li^+ ions and layers of non-magnetic Cu^+ sites. One key element of the present work was the preparation of samples with a thoroughly controlled chemical composition. Single crystals of LiCu_2O_2 were grown in an alundum crucible in air atmosphere using the self-flux method. The

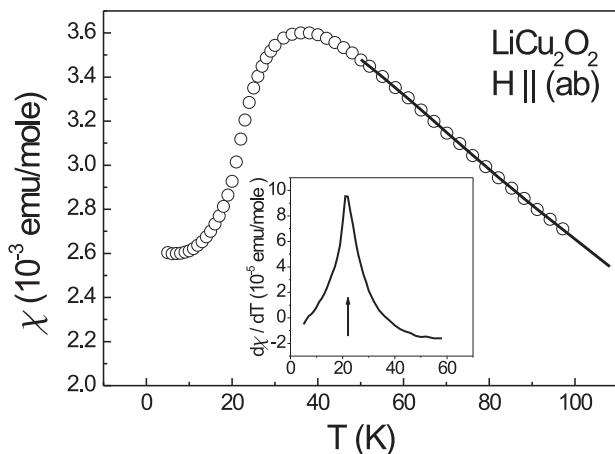


FIG. 2: Temperature dependence of magnetic susceptibility of LiCu_2O_2 measured in a magnetic field $H = 100$ Oe applied parallel to the (a, b) cleavage plane (symbols). The solid line is a fit based on the frustrated $S = 1/2$ chain model, as described in the text. Taking a numerical derivative (inset) reveals a phase transition $T_c = 22$ K (arrow).

lattice parameters $a = 5.730(1)\text{\AA}$, $b = 2.8606(4)\text{\AA}$, and $c = 12.417(2)\text{\AA}$ were verified by powder X-rays diffraction, which also confirmed the absence of any appreciable amounts of impurity phases. These values are in very good agreement with those reported in [8]. All crystals were found to be microscopically twinned with respect to the $[1, 1, 0]$ plane, so that $a \approx 2b$.

Unexpectedly, it was found that those samples with the smallest mosaic spread and most reproducible magnetic behavior had lower content of Cu^+ ions than follows from the stoichiometric formula $\text{Li}_1+\text{Cu}_2+\text{O}_2$. The density was determined to be $\rho = 5.12$ g/cm³ at room temperature, which corresponds to an actual composition $\text{Li}_{1.16}\text{Cu}_{1.84}\text{O}_{2.01}$. Chemical disorder and a Cu-deficiency by as much as $x = 16\%$ are thus inherently present. The “surplus” Li^+ ions in $\text{Li}_{1.16}\text{Cu}_{1.84}\text{O}_{2.01}$ occupy Cu^{2+} sites, due to a good match of ionic radii. A substitution of Cu^+ ions by Li^+ ions in the LiCu_2O_2 structure is prevented by the dumbbell oxygen coordination being very uncharacteristic for the latter ion type. Charge compensation requires that the introduction of 16% non-magnetic Li^+ ions into the double chains is accompanied by a transfer of 16% of the $S = 1/2$ -carrying Cu^{2+} ions onto the Cu^+ inter-chain sites. As will become crucial for the discussion below, our *disordered and non-stoichiometric* $\text{Li}_{1.16}\text{Cu}_{1.84}\text{O}_{2.01}$ crystals (referred to as simply “ LiCu_2O_2 ” throughout the rest of the paper) have appreciable concentrations of both *non-magnetic* Li^+ impurities in the zig-zag chains, and *magnetic* Cu^{2+} impurities positioned in-between chains.

The single crystal samples were characterized by bulk susceptibility and specific heat measurements. $\chi(T)$ data were taken in a commercial SQUID magnetome-

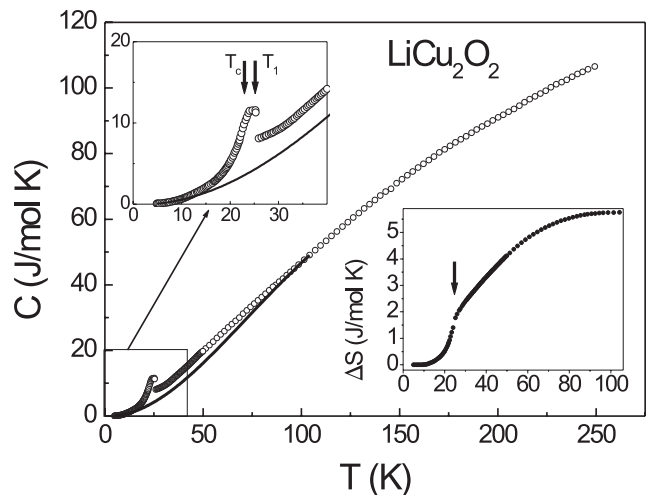


FIG. 3: The measured temperature dependence of specific heat in LiCu_2O_2 (open symbols) indicates a phase transition at $T_c \approx 22$ K and a possible precursor at $T_1 \approx 25$ K (arrows). Subtracting the phonon contribution (solid line) allows to extract the temperature dependence of magnetic entropy (lower right inset).

ter in the temperature range 5–100 K and a magnetic field $H = 100$ Oe applied parallel to the (a, b) cleavage plane and are shown in symbols in Fig. 2. The main feature is a broad maximum at $T \approx 36$ K characteristic of a quasi-one-dimensional magnet, that signifies the formation of short-range correlations within the chains. Taking the temperature derivative of the magnetic susceptibility (Fig. 2, inset) reveals a sharp anomaly at $T_c = 22$ K, that we attribute to the onset of long-range magnetic order. The high-temperature part of the $\chi(T)$ curve is expected to be uninfluenced by this phase transition, representing the behavior of individual zig-zag chains. The data taken above $T = 50$ K were analyzed using the high-temperature expansion formulas for the susceptibility of the quantum $S = 1/2$ frustrated-chain model [9]. An excellent fit (solid line in Fig. 2) is obtained with $J_1 = 5.9(1)$ meV, $g = 2.114(2)$, and $\alpha = 0.282(3)$. The anomaly at T_c is also manifest in the specific heat data measured using a “Termis” quasiadiabatic microcalorimeter and plotted in Fig. 3. The peak observed at $T \approx T_c$ is well-defined, but, as indicated by arrows in the blowup plot, actually has a characteristic flat top that extends between $T_c = 22$ K and $T_1 = 24$ K, in agreement with the results of Ref. [7]. The solid line in Fig. 3 represents a crude estimate for the phonon contribution, calculated under the assumption that the total magnetic entropy released at short-range and long-range ordering in LiCu_2O_2 is equal to $R \ln(2S + 1) = 5.76$ J/mole K. The temperature dependence of magnetic entropy extracted in this fashion is plotted in the lower right inset of Fig. 3. A large fraction of the entropy is released above the ordering temperature,

as expected for a low-dimensional system. The sharp 9 K anomaly reported in Ref. [6] is totally absent in our $\chi(T)$ and $C(T)$ data. We suspect that this feature is due to an impurity phase, most likely Li_2CuO_2 , which is known to go through an AF transition at 9 K [10]. Otherwise, the characteristics of our samples seem to be in good agreement with those reported by other authors [3, 4, 5, 7].

The nature of the magnetically ordered state was determined in a single-crystal neutron diffraction experiment. Since LiCu_2O_2 was prepared using a naturally occurring Li isotope mixture, the attenuation of a neutron beam due to absorption by ^6Li nuclei was significant. The sample was cut parallel to the (a, b) crystallographic plane to the shape of a thin plate $0.9 \times 15 \times 15 \text{ mm}^3$. The measurements were performed at the HB1 and HB1A 3-axis spectrometers installed at the High Flux Isotope Reactor at ORNL. For measuring integrated Bragg intensities the instruments were used in 2-axis mode, with a well-collimated incident neutron beam of a fixed energy $E_i = 14.7 \text{ meV}$. A Pyrolytic Graphite PG(002) reflection was used in the monochromator. A 5 cm thick PG filter was positioned in front of the sample to eliminate higher-order beam contamination. Bragg intensities were collected in rocking curves and corrected for the usual Lorentz factor. Absorption corrections were applied assuming a thin-plate geometry. High-resolution measurements of the magnetic propagation vector were performed in 3-axis mode, with a PG(002) analyzer and $48' - 40' - 40' - 240'$ collimators.

The main finding of this work is that below $T_c \approx 22 \text{ K}$ LiCu_2O_2 acquires *incommensurate* magnetic long range order [18]. The phase transition leads to the appearance of new Bragg reflections that can be indexed as $(\frac{2n+1}{2}, k \pm \eta, l)$, n, k, l -integer, $\zeta \approx 0.174$. Such peaks were observed in both crystallographic twins. The peak widths were found to be resolution-limited along all three crystallographic directions at all temperatures below T_c . A typical scan across the $(0.5, 0.826, 0)$ reflection taken at $T = 2 \text{ K}$ is shown in the inset of Fig. 4a. The corresponding peak intensity is plotted as a function of temperature in Fig. 4a. A simple power law fit to the data taken above $T = 15 \text{ K}$ yields $T_c = 22.3(6) \text{ K}$ and $\beta = 0.25(0.07)$. The residual intensity seen in Fig. 4a at $T > T_c$ is due to critical scattering and is quite broad in q -space.

The temperature dependence of the magnetic propagation vector was deduced from Gaussian fits to k -scans across the $(0.5, 0.826, 0)$ peak, and is plotted in symbols in Fig. 4b. Below $T \approx 17 \text{ K}$ the incommensurability parameter is practically T -independent and appears to have a strictly incommensurate value $\zeta = 0.1738(2)$. Interestingly, as T_c is approached from below, ζ progressively decreases as indicated by the arrow in Fig. 4b. The minimum value of ζ observed in our experiments is about 0.172. The temperature dependence of ζ may be the cause for a flat-top peak in the measured specific heat curve. In the close vicinity of T_c , where ζ changes rapidly,

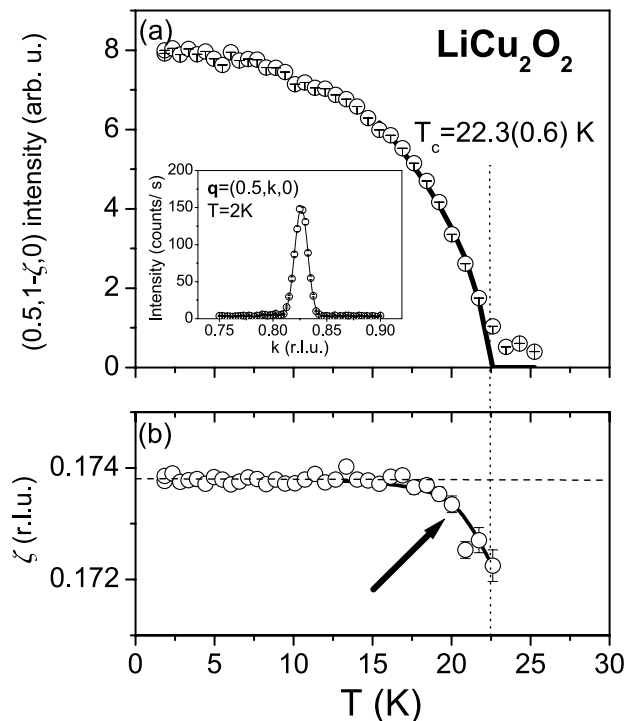


FIG. 4: (a) Measured temperature dependence of the $(0.5, 0.826, 0)$ magnetic peak intensity in LiCu_2O_2 (symbols). The solid line is a power law fit to the data. Inset: k -scan across this reflection measured at $T = 2 \text{ K}$. (b) Measured incommensurability parameter ζ plotted as a function of temperature. The solid line is a guide for the eye.

the large-period structure may undergo one or more “devil’s staircase”-type commensuration transitions, particularly at T_1 [7]. Intensity being the limiting factor, we were unable to locate any well-defined magnetic Bragg reflections in the narrow temperature range $T_c < T < T_1$.

The spin arrangement in the ordered state was deduced from the analysis of 23 non-equivalent magnetic Bragg peaks with $0 \leq h \leq 3.5$, $0 \leq k \leq 1.5$ and $0 \leq l \leq 8$. Those reflections for which the incident or scattered beams formed angles of less than 15° with the crystalline plate were not included in this data set, since the corresponding absorption corrections are expected to deviate substantially from the thin-plate approximation. After examining a number of models, we found that excellent fits to the data are obtained assuming a planar spin-helix propagating along the zig-zag Cu^{2+} chains, with a fixed relative rotation angle $\phi = \pi(1 - \zeta)$ between consecutive spins. Any spins related by a translation along the c axis and b axes are parallel and antiparallel to each other, respectively. The magnetic structure factor for such a helical state can be easily calculated analytically [11]. After averaging over possible q -domains and taking into account the magnetic form factor of Cu^{2+} , an excellent fit to the measured magnetic intensities is obtained assuming all spins to be confined to the (a, b)

crystallographic plane, and adjusting only an overall intensity scaling factor. This spin structure is visualized in Fig. 1. Unfortunately, an independent estimate of the magnitude of the ordered moment from our data was prevented by rather severe extinction corrections of nuclear Bragg intensities typically used for normalization.

A helimagnetic state is the typical way geometric frustration is resolved in a classical magnet. Perhaps the first of many known examples is that of MnO_2 , dating back to the 50's [12]. The incommensurability parameter ζ is directly related to the frustration ratio α through $4\alpha = 1/\cos(\pi\zeta)$. In our case, for $\zeta = 0.174$ this yields $\alpha = 0.29$, in excellent agreement with our estimates based on high-temperature bulk susceptibility data. What makes LiCu_2O_2 remarkable, is that according to existing theories for *quantum* $S = 1/2$ spin chains with nnn interactions, this value corresponds to a *gapped disordered dimer-liquid state*, not too far from the collinear gapless phase realized for $\alpha < 0.241$ [13]. This would seem to agree well with the observation of a spin gap at $T > T_c$ [6], but is of course incompatible with incommensurate long-range order at lower temperatures. One possible explanation for the observed behavior are strong inter-chain interactions, such as those that induce ordering in the well understood Haldane-gap compound CsNiCl_3 [14]. Here the amplitude of transverse dispersion of the energy gap increases with decreasing T , eventually driving the gap to zero at the 3D zone-center and inducing a soft-mode phase transition. A similar mechanism may be active in LiCu_2O_2 , and is not incompatible with the ESR data of Ref. [6]. Nevertheless, it is difficult to envision the necessary strong inter-chain superexchange pathways in the stoichiometric material.

Chemical disorder, that is *inherently present in our samples* may be expected to play an important role in magnetic ordering. In particular, the 16% Li^+ *non-magnetic* defects in the double chains will locally destroy valence bond spin-singlets and liberate end-chain spin degrees of freedom. The free spins can then order in three dimensions via arbitrary small inter-chain interactions. This mechanism is known to drive magnetic ordering in the spin-Peierls compound CuGeO_3 [15], and the Haldane-gap system $\text{PbNi}_2\text{V}_2\text{O}_8$ [16]. Alternatively, long-range ordering in LiCu_2O_2 may be driven by the 16% Cu^{2+} impurities positioned in-between the gapped spin chains. Such *magnetic* impurities carry interactions across the non-magnetic Cu^+ layers, completing a 3D network of magnetic interactions. Long range order occurs for an arbitrary small concentration of impurities, and involves ordering of both the impurity spins and the chain spins. This model is realized in $(R_x\text{Y}_{1-x})_2\text{BaNiO}_5$ rare earth nickelates, where classical R^{3+} ions bridge the Ni-based gapped spin chains [17]. To fully understand the role of impurities in the ordering of LiCu_2O_2 more detailed neutron scattering experiments on isotopically pure samples are required.

In summary, we have observed incommensurate helimagnetism in a $S = 1/2$ zig-zag chain compound where the estimated frustration ratio corresponds to gapped disordered phase. We speculate that long-range magnetic ordering is aided by intrinsic impurities and deviations from stoichiometry. This work was partially supported by RFBR Grants 02-02-17798 and 03-02-16108. Work at ORNL was carried out under DOE Contract No. DE-AC05-00OR22725.

-
- [1] C. K. Majumdar and D. K. Ghosh, J. Math. Phys. **10**, 1388 (1969); B. S. Shastry and B. Sutherland, Phys. Rev. Lett. **47**, 964 (1981); F. D. M. Haldane, Phys. Rev. B **25**, 4925 (1982); S. R. White and I. Affleck, Phys. Rev. B **54**, 9862 (1996); A. A. Aligia, C. D. Batista and F. H. L. Essler, Phys. Rev. B **62**, 3259 (2000) and references therein.
 - [2] A. A. Nersisyan and F. H. L. Essler, Phys. Rev. Lett. **81**, 910 (1998).
 - [3] A. M. Vorotynov *et al.*, JETP **86**, 064424 (1998); J. Magn. magn. Mater. **188**, 233 (1998).
 - [4] F. Fritschij, H. Brom, and R. Berger, Solid State Commun. **107**, 719 (1998).
 - [5] A. A. Zatsopin *et al.*, Phys. Rev. B **57**, 4377 (1998).
 - [6] S. Zvyagin *et al.*, Phys. Rev. B **66**, 064424, (2002).
 - [7] B. Roessli *et al.*, Physica B **296**, 306 (2001).
 - [8] R. Berger, J. Less-Common Met. **169**, 33 (1991); R. Berger, P. Onnerund and R. Tellgren, J. Alloys Compd. **184**, 315 (1992).
 - [9] G. S. U. A. Buhler, N. Elstner, Eur. Phys. J. B **16**, 475 (2000).
 - [10] M. Boehm *et al.*, Europhys. Lett. **43**, 77 (1998).
 - [11] A. Furrer (Ed.), Magnetic Neutron Scattering, Part I, Chapter 5, World Scientific Publishing (1995).
 - [12] R. A. Erickson, Phys. Rev. **85**, 745 (1952); A. Yoshimori, J. Phys. Soc. Jpn. **14**, 807 (1959).
 - [13] T. Tonegawa and I. Harada, J. Phys. Soc. Jpn. **56**, 2153 (1987); K. Okamoto and K. Nomura, Phys. Lett. A **169**, 433 (1992); R. D. Somma and A. A. Aligia, Phys. Rev. B **64**, 024410 (2001).
 - [14] W. J. L. Buyers *et al.*, Phys. Rev. Lett. **56**, 371 (1986); R. M. Morra *et al.*, Phys. Rev. B **38**, 543 (1988).
 - [15] M. Hase *et al.*, Phys. Rev. Lett. **71**, 4059 (1993); T. Masuda *et al.*, Phys. Rev. Lett. **80**, 4566 (1998).
 - [16] Y. Uchiyama *et al.*, Phys. Rev. Lett. **83**, 632 (1999); Physica B **284-288**, 1641 (2000); A. Zheludev *et al.*, Phys. Rev. B **64**, 134415(2001); A. I. Smirnov *et al.*, Phys. Rev. B **65**, 174422 (2002).
 - [17] A. Zheludev *et al.*, Phys. Rev. Lett. **80**, 3630 (1998); S. Maslov and A. Zheludev, Phys. Rev. Lett. **80**, 5786 (1998); A. Zheludev *et al.* J. Phys.: Condens. Matter **13**, R525 (2001).
 - [18] While preparing this manuscript, we became aware of an independent unpublished NMR study by A. A. Gippius, E. N. Morozova, A. S. Moskvina, A. V. Zalessky, A. A. Bush, M. Baenitz and S.-L. Drechsler, that contains additional evidence of incommensurability in LiCu_2O_2 , but provides no specific information on the magnetic structure, frustration ratio or the role of non-stoichiometry.

